Alumina-Supported Gallium Oxide Catalysts for NO Selective Reduction: Influence of the Local Structure of Surface Gallium Oxide Species on the Catalytic Activity

Ken-ichi Shimizu,*,† Mikio Takamatsu,† Koji Nishi,† Hisao Yoshida,† Atsushi Satsuma,† Tsunehiro Tanaka,‡ Satohiro Yoshida,‡ and Tadashi Hattori*,§

Department of Applied Chemistry, Graduate School of Engineering, Nagoya University, Chikusa-ku, Nagoya 464-8603, Japan, Department of Molecular Engineering, Graduate School of Engineering, Kyoto University, Sakyo-ku, Kyoto 606-8501, Japan, and Research Center for Advanced Waste and Emission Management, Nagoya University, Chikusa-ku, Nagoya 464-8603, Japan

Received: September 21, 1998; In Final Form: December 23, 1998

The surface structure of alumina-supported gallium oxide catalysts for selective catalytic reduction of NO by CH_4 was studied. The XPS results showed that Ga atoms were dispersed well over the Al_2O_3 surface for the samples with Ga_2O_3 content below monolayer coverage (27 wt %) and that Ga_2O_3 particles appeared at higher content. The XANES and EXAFS results revealed that, below monolayer coverage, Ga atoms were located at the surface cation sites (tetrahedral and octahedral) of Al_2O_3, and the fraction of tetrahedral Ga species decreased as Ga content increased. The activity per surface area of the catalysts increased with Ga_2O_3 content up to around the monolayer coverage and declined at higher content. Below monolayer coverage, the activity per exposed Ga atom decreased as Ga content increased, which correlated well with the change in the fraction of tetrahedral Ga species. It was concluded that the present reaction is a structure-sensitive reaction depending on the local structure of Ga atom; GaO_4 tetrahedra highly dispersed in the surface spinel are responsible for the activity.

Introduction

The selective catalytic reduction (SCR) of nitrogen oxides by hydrocarbons has attracted much attention as a new type of de-NO_x process.[1−3] In particular, SCR by CH_4 is most challenging since CH_4 is relatively inert and generally reacts with O_2 much faster than with NO thermally and over most catalysts.[3] SCR by CH_4 is also of practical importance since it has the potential ability to remove NO_x from stationary engines at the power plants, where CH_4 is commonly used as a fuel.[3] So far, most of the effective catalysts for SCR by CH_4 reported are metal-exchanged zeolites,[2−5] and among them Ga-ZSM-5 is of interest because of its extraordinary high selectivity.[4,5] On the other hand, oxide catalysts such as Al_2O_3, which are expected to be more stable hydrothermally, were known to be less active than zeolitic ones.[4,5] However, we have recently demonstrated that Ga_2O_3/Al_2O_3 showed high activity and selectivity as comparable to Ga-ZSM-5 for SCR by CH_4, implying that it is not essential to use zeolite as a matrix for this reaction.[6] In addition, Ga_2O_3/Al_2O_3 showed higher tolerance against water than Ga-ZSM-5, which indicates the possibility of designing de-NO_x catalysts with high durability by using a nonzeolitic matrix.[6]

Many of the SCR catalysts consist of metal cations as an active center and an oxide support, such as ZSM-5 or Al_2O_3, and hence the role of support is one of the major concerns. The support is shown to play a role in dispersing active species for this reaction.[6−8] It can also participate in certain steps in the reaction, and many contributions have been devoted to this aspect, so-called "bifunctionality".[5,9,10] Besides these roles, the support can affect the chemical nature of the active component, and thus influence the catalytic activity. Previously, we have reported that the activity of Ga_2O_3 catalysts for NO reduction by CH_4 are greatly influenced by the support; gallium oxide on Al_2O_3 exhibited the highest intrinsic activity, and it has a specific local structure different from bulk oxides.[11] However, the detailed structure of the active gallium species still remains to be solved.

This paper is intended to investigate the influence of the coordination symmetry and surrounding matrix of the surface gallium species on the catalytic activity of Ga_2O_3/Al_2O_3 catalysts. First, we studied the surface structure of Ga_2O_3/Al_2O_3 as a function of Ga_2O_3 content by XPS and X-ray absorption spectroscopy (XANES and EXAFS). Deconvolution analysis of XANES, which we have recently developed,[12] was applied to the quantification of gallium coordinations (tetrahedral and octahedral). Second, the activity of Ga_2O_3/Al_2O_3 in the NO reduction by CH_4 was studied from the standpoint of structure sensitivity. The results obtained by the structural analysis explain the dependence of the catalytic activity on Ga_2O_3 content, and the local structure of the active species required for this reaction is discussed.

Experimental Section

Materials. Ga_2O_3/Al_2O_3 catalysts were prepared by impregnation of Al_2O_3 (a reference catalyst of the Catalysis Society of Japan,[13] JRC-ALO-1A, γ-type, 160 m^2/g) with aqueous

* Corresponding authors.
† Department of Applied Chemistry, Graduate School of Engineering, Nagoya University.
‡ Department of Molecular Engineering, Graduate School of Engineering, Kyoto University.
§ Research Center for Advaned Waste and Emission Management, Nagoya University.

10.1021/jp983790w CCC: $18.00
Published on Web 02/17/1999

solutions of gallium nitrate, followed by evaporation to dryness at 393 K, and calcining in air for 4 h at 823 K. Reference compounds were obtained as follows. β-Ga_2O_3 was purchased from Mitsuwa Chemicals. $Ga(acac)_3$ was purchased from Aldrich. MFI-type gallosilicate zeolite (Ga-MFI) containing a small amount of Ga (Si/Ga = 80) in the framework was synthesized hydrothermally and calcined at 823 K for 4 h.[12] $Ga_2O_3-Al_2O_3$ mixed oxide (1/4 in Ga/Al atomic ratio) was prepared from their nitrate salts using aqueous ammonia as the precipitation agent. The precipitate was dried at 395 K and calcined in air for 4 h at 1073 K. BET surface areas of the samples were determined using nitrogen adsorption. The X-ray diffraction pattern of the powdered catalysts was recorded with a Rigaku RINT 1200 diffractometer.

XPS. XPS measurements were performed with an AXIS-HSi photoelectron spectrometer using Al Kα radiation (1485.9 eV). To examine the extent of dispersion of Ga on Al_2O_3, a quantitative analysis of XPS data has been performed as follows on the basis of the previous studies.[14,15] When an Al_2O_3 surface is covered by a uniform Ga_2O_3 monolayer of thickness d and coverage θ and the electron takeoff angle is taken at 90° from the surface plane, the intensity ratio of the Ga $3p_{3/2}$ to the Al 2s can be expressed as follows:

$$\frac{I_{Ga}}{I_{Al}} = \frac{\sigma_{Ga}\lambda_{Ga,Ga}n_{Ga}\,\theta[1-\exp(-d/\lambda_{Ga,Ga})]}{\sigma_{Al}\lambda_{Al,Al}n_{Al}[1-\theta+\theta\exp(-d/\lambda_{Al,Ga})]} \quad (1)$$

$$\theta = N_{Ga}/(N\cdot S) \quad (2)$$

where I_{Ga} and I_{Al} represent the XPS intensities of Ga $3p_{3/2}$ and of Al 2s, respectively; $\lambda_{Ga,Ga}$ (1.52 nm), $\lambda_{Al,Al}$ (1.82 nm), and $\lambda_{Al,Ga}$ (1.83 nm) are the escape depths[16] of the photoelectrons from Ga $3p_{3/2}$ through Ga_2O_3, that from Al 2s through Al_2O_3, and that from Al 2s through Ga_2O_3, respectively; σ_{Ga} (2.11) and σ_{Al} (0.75) are the ionization cross sections[17] for Ga and Al, respectively; n_{Ga} (37.1 nm^{-3}) and n_{Al} (40.1 nm^{-3}) are the number densities of the Ga atom in β-Ga_2O_3[18] and the Al atom in γ-Al_2O_3,[19] respectively; d (0.3 nm) is the thickness of an ideal (100) monolayer of β-Ga_2O_3.[18] θ can be expressed by eq 2, where N_{Ga}, N, and S are the number of Ga atoms loaded on Al_2O_3, the number of surface cation sites on Al_2O_3 support calculated from the cation site density of (111) face of γ-Al_2O_3 (14.5 Al nm^{-2}),[20] and the surface area of the support, respectively.

X-ray Absorption. Ga K-edge XAFS spectra were recorded at BL-10B[21] of the Photon Factory in High-Energy Accelerator Research Organization, Tsukuba, Japan, with a ring energy of 2.5 GeV and stored current of 250−350 mA. The spectra were recorded in a transmission mode at room temperature with a Si(311) channel cut monochromator (d = 1.6375 Å). The intensities of the incident and transmitted X-rays were measured with a 17-cm ion chamber with a flowing gas mixture of N_2 (85%) and Ar (15%) and a 31-cm ion chamber with a flowing gas mixture of N_2 (75%) and Ar (25%), respectively. The estimated resolution was about 1 eV at around Ga K-edge (10371 eV).[21] The data were collected with an energy step of ca. 0.5 eV at 10371 eV. Normalization of XANES and data reduction and curve-fitting analysis of EXAFS were carried out as described elsewhere.[12]

Selective Reduction of NO. Catalytic activity tests were carried out using a fixed-bed flow reactor at atmospheric pressure.[6] The reaction mixture consisted of 1000 ppm NO, 1000 ppm CH_4, and 6.7% O_2; the total flow rate was 42 mL min^{-1} over 0.04−0.5 g catalysts. After reaching steady-state conditions, effluent gas was analyzed by gas chromatography and by an NO_x analyzer. Near 100% carbon balance and nitrogen balance were obtained. The rate of NO reduction to N_2 was measured under differential conditions where NO and CH_4 conversions were below 30%.

TABLE 1: Physical Characteristics of Ga_2O_3/Al_2O_3 Catalysts

Ga_2O_3 content/wt %	surface area[a]/m^2g^{-1} catalyst	surface area[b]/m^2g^{-1} Al_2O_3	crystal phase of Ga_2O_3[c]
0	160	160	
3	158	162	
7	153	164	
13	147	170	
21	129	163	
27	129	176	
36	130	203	ϵ
44	122	215	ϵ
60	100	217	ϵ
77	93	402	ϵ
100[d]	71	−	ϵ

[a] BET surface area per gram of catalyst. [b] BET surface area per gram of Al_2O_3 support. [c] Determined by X-ray diffraction. [d] Prepared by calcination of gallium nitrate at 823 K for 4 h.

Results

Physical Characteristics. Table 1 lists the BET surface areas and crystal phases of the catalysts. XRD patterns of the samples with Ga_2O_3 content below 27 wt % showed lines due to γ-Al_2O_3 support, but not lines due to Ga_2O_3. Small lines due to ϵ-Ga_2O_3 were detected on a 36 wt % sample, and their intensity increased as the Ga_2O_3 content increased. A Ga_2O_3 sample prepared by calcining gallium nitrate at the same calcination condition as Ga_2O_3/Al_2O_3 samples also exhibited ϵ-Ga_2O_3 phase.[12] The surface area per gram of Al_2O_3 support was calculated by subtracting out the mass contributed by gallium assumed to be in the form of Ga_2O_3. The value remains fairly constant (169 ± 7 m^2 g^{-1}) up to about 27 wt % Ga_2O_3, suggesting that Ga_2O_3 on Al_2O_3 is present as a thin-layer structure. At a higher Ga_2O_3 content, a systematic increase in the surface area per gram of Al_2O_3 was observed as the Ga_2O_3 content increased, probably due to the formation of Ga_2O_3 particles.

XPS. Figure 1 shows the Ga $3p_{3/2}$/Al 2s XPS intensity ratio as a function of the Ga_2O_3 content. The intensity ratio increased linearly with Ga_2O_3 content up to 27 wt %. At higher Ga_2O_3 content there was a drastic enhancement of the intensity ratio. A linear relationship between the XPS intensity ratio and the content can be obtained for monolayer catalysts as reported by Fung[14] in the WO_3/Al_2O_3 system and by Hercules et al.[22] in the Co/Al_2O_3 system. The theoretical line for monolayer dispersion is calculated from eq 1 and is shown in Figure 1 (dotted line). The ratios I_{Ga}/I_{Al} experimentally obtained were very consistent with the calculated value up to at least 27 wt %. These results suggest that Al_2O_3 surface is covered with a uniform gallia layer of thickness much less than the escape depth up to around 27 wt %. The change in slope at high content indicates that an alteration in the surface composition has taken place at around 27 wt %.

Ga K-Edge XANES. Figure 2 shows X-ray absorption near-edge structures (XANES) around the Ga K-edge for the samples together with those of some reference compounds of known structure. As a reference compound for octahedral Ga^{3+} species, $Ga(acac)_3$ was employed since the six oxygen atoms form a nearly ideal octahedron.[23] The XANES spectra of $Ga(acac)_3$ exhibited a peak at 10379 eV. Ga-MFI was used as a reference compound for tetrahedral Ga^{3+} species.[24] The XANES spectra

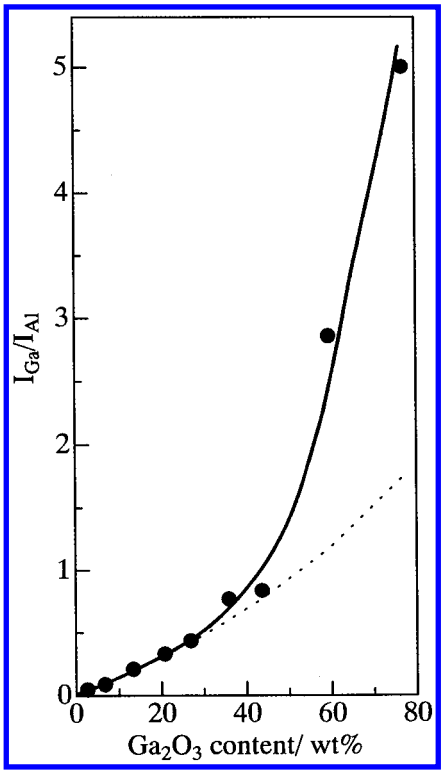

Figure 1. XPS Ga $3p_{3/2}$/Al 2s intensity ratio as a function of Ga_2O_3 content; the dotted line denotes the theoretical Ga $3p_{3/2}$/Al 2s intensity ratio calculated for monolayer dispersion.

of Ga-MFI exhibited a peak at 10375 eV. In our previous study, the peaks at 10379 and at 10375 eV were assigned to octahedral Ga species, Ga(o), and tetrahedral Ga species, Ga(t), respectively.[12] β-Ga_2O_3 was also used as a model in which Ga atoms are equally distributed between tetrahedral and octahedral sites of the spinel.[18] The XANES spectra of β-Ga_2O_3 exhibited an absorption maximum at 10379 eV with a shoulder at about 10375 eV, which are due to Ga(o) and Ga(t), respectively.[12]

As shown in Figure 2, XANES spectra of the Ga_2O_3/Al_2O_3 samples exhibited peaks at 10375 and at 10379 eV, which are due to Ga(t) and Ga(o), respectively. Small peaks at 10385 eV also appeared in the post-edge region, but it was not employed for the analysis.[12] The XANES spectra of the low-content samples were characteristic of strong peak at 10375 eV due to Ga(t), and were close to that of $Ga_2O_3-Al_2O_3$ mixed oxide. As Ga_2O_3 content increased, the intensity of the peak at 10375 eV decreased, while that of the peak at 10379 eV increased. At the highest content (77 wt %), the feature of the spectrum was similar to that of ϵ-Ga_2O_3, in which the 10379 eV peak due to Ga(o) was predominant. It is likely that the local structure of Ga atoms in Ga_2O_3/Al_2O_3 varies with Ga_2O_3 content; the ratio of Ga(t) to Ga(o) decreases as Ga_2O_3 content increases.

In our previous study,[12] the deconvolution analysis of XANES spectra was performed for gallium oxides; the normalized XANES spectrum of β-Ga_2O_3 was deconvoluted to two arctangent curves for continuum absorption and two Gaussian curves for the white line, and it was clarified that the ratio of Ga(t)/Ga(o) can be estimated quantitatively from the ratio of each peak area. In this study, the same method was applied to the Ga_2O_3/Al_2O_3 samples to obtain the fraction of Ga(t) and Ga(o) species. The deconvoluted spectrum of 21 wt % Ga_2O_3/Al_2O_3 is illustrated in Figure 3 as an example. The result of the deconvolution analysis for the samples was listed in Table 2. The positions of two Gaussian peaks were centered at 10375.2 $\pm$ 0.5 eV and 10379.1 $\pm$ 0.7 eV, which were almost identical

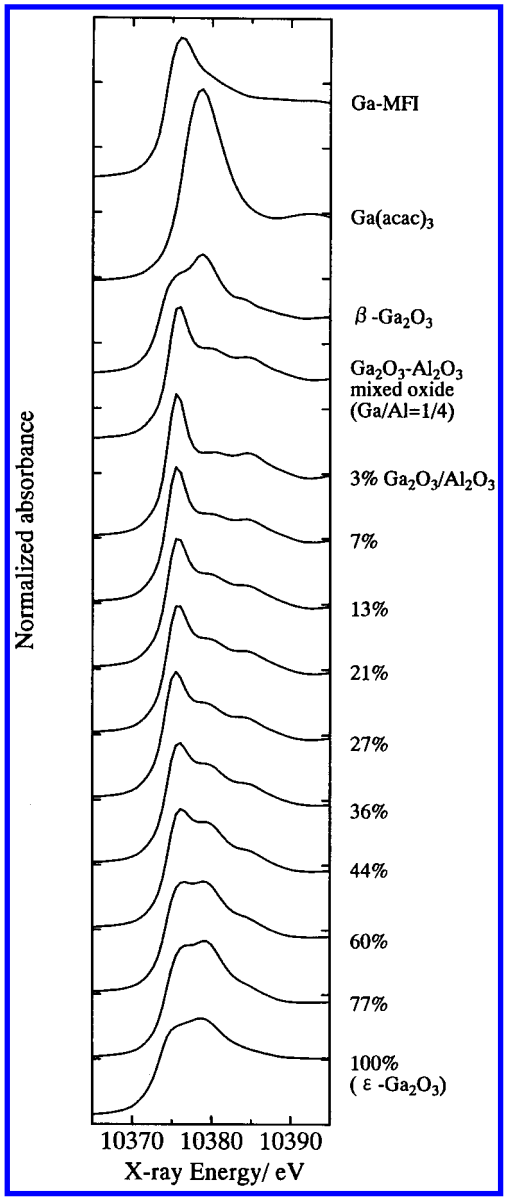

Figure 2. Ga K-edge XANES spectra of Ga_2O_3/Al_2O_3 catalysts and reference compounds.

to those of Ga(t) and Ga(o), respectively. The sum of the peak areas due to Ga(t) and Ga(o) was almost constant (7.4 $\pm$ 0.7 eV unit) for the Ga_2O_3/Al_2O_3 samples. It follows that the fractions of Ga(t) and Ga(o) can be estimated from the fractions of each peak area. The fractions thus estimated are plotted in Figure 4 as a function of Ga_2O_3 content. It was clearly shown that, as Ga_2O_3 content increased, the fraction of Ga(t) decreased, while that of Ga(o) increased.

EXAFS. The k^3-weighted EXAFS of reference compounds and Ga_2O_3/Al_2O_3 samples are shown in Figure 5A. Fourier transform was performed on these EXAFS in the 5.0−15.5 $Å^{-1}$ region, and the radial structure function (RSF) was obtained as shown in Figure 5B. Peaks at 1−2 Å are due to the backscattering from the adjacent oxygen atoms, and peaks at 2−4 Å show the presence of the second-neighboring metal atoms (Ga or Al). The positions of the Ga−O shell of reference compounds were 1.45 Å for Ga-MFI and 1.65 Å for Ga(acac)$_3$, which agrees with the fact that the average Ga−O distance of Ga-MFI, 1.78 Å,[24] is shorter than that of Ga(acac)$_3$, 1.95 Å.[23] The peak positions of the Ga−O shell for the Ga_2O_3/Al_2O_3 samples were lower than that for Ga-MFI. As for the second shell, an intense peak due to the Ga−Ga shell was centered at 2.8 Å for β-Ga_2O_3.

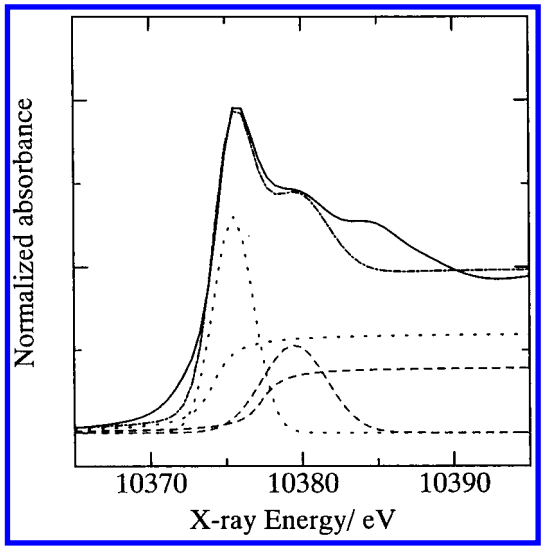

Figure 3. Ga K-edge XANES spectrum of 21 wt % Ga_2O_3/Al_2O_3 (solid line) and the simulated spectrum (−•−) which is composed of two sets of a Gauss and an arctangent functions (dotted and broken).

While, for the Ga_2O_3/Al_2O_3 sample of 3 wt %, the position of the Ga−M shell was 3.0 Å, which was higher than that for β-Ga_2O_3, and slightly shifted to the lower value as the Ga_2O_3 content increased.

The inverse Fourier transform of the first shell (R = 0.68−2.0 Å) and the second shell (R = 2.0−3.8 Å) in the RSF gives the Fourier-filtered EXAFS function due to the Ga−O and the Ga−M (M = Ga or Al) shown in Figure 6, partsA and B, respectively (solid lines). It is well-known that magnitude of an EXAFS envelope function is high in the region of relatively high k when the surrounding atoms are heavy atoms.[26] For β-Ga_2O_3, the amplitude in the k region of 9−11 $Å^{-1}$ was intense and the maximum of the envelope was observed at around 10.2 $Å^{-1}$, which is a typical phenomenon for backscattering from heavy atoms, i.e., Ga atoms. On the other hand, the maximum was observed at around 6.5 $Å^{-1}$ for the sample of 3 wt %, which indicates the presence of a light atom, i.e., an Al atom, as the adjacent metal atom. As Ga_2O_3 content increased, the maximum of the envelope shifted slightly to the higher value, which indicates an increasing number of the heavy component, Ga atom, around Ga atom.

The structural parameters were evaluated by the curve-fitting analysis. For the first shell due to the Ga−O, the curve-fitting was carried out in the k region of 5.0−14.0 $Å^{-1}$. Since the average Ga−O distance in β-Ga_2O_3 varies with coordination symmetry (1.83 Å for Ga(t)-O, and 2.00 Å for Ga(o)-O),[18] two-shell fitting was used for the first shell, and we assumed the Ga−O shell with shorter bond distances to be Ga(t)−O and that with longer bond distances to be Ga(o)−O as mentioned in our previous study.[12] The employed amplitudes and phase shifts for Ga(t)−O and Ga(o)−O pairs were empirical ones extracted from the EXAFS of Ga-MFI and $Ga(acac)_3$, respectively. It should be noted that the alternative model with a single shell has resulted in poorer fits. For the second shell due to Ga−M, taking into account the above results that both Ga and Al can be present as adjacent metal atoms, it seems reasonable to perform the curve-fitting with the two shells of Ga−Ga and Ga−Al. Since compounds where regular coordination of Ga atoms with Ga and Al atoms were not available, theoretical phase shifts and amplitudes for Ga−Ga and Ga−Al pairs taken from FEFF (6)[27] were used. As shown in Figure 6, parts A and B, simulated spectra (dotted line) fitted well with the experimental ones.

Table 3 summarizes the curve-fitting results of β-Ga_2O_3 and the Ga_2O_3/Al_2O_3 samples. The result of β-Ga_2O_3 shows that EXAFS data are in good agreement with the corresponding crystallographic parameters,[18] which confirms that the fitting procedure was successful. For the Ga_2O_3/Al_2O_3 samples, the bond distances of Ga(t)−O and Ga(o)−O were almost constant for the samples below 27 wt % (R_t = 1.70 Å and R_o = 1.88 Å), and were shorter than those for β-Ga_2O_3 (R_t = 1.86 Å and R_o = 2.02 Å). For the samples above 36 wt %, the bond distances increased as Ga_2O_3 content increased. The coordination number of the Ga(t)−O shell increased with an increase in Ga_2O_3 content, whereas that of the Ga(o)−O shell decreased. By using the coordination numbers for each shell, N_t and N_o, the fraction of Ga(t) species can be estimated and was included in Table 3. As for the second shell, the interatomic distances of Ga−Ga and Ga−Al were almost constant within an error for all the samples (3.20 ± 0.02 Å for Ga−Ga, and 3.32 ± 0.02 Å for Ga−Al). The coordination number of the Ga−Ga shell was the lowest (N = 0.4) for a sample of 3 wt % and increased with an increase of Ga_2O_3 content, whereas that of the Ga−Al shell was highest (N = 7.2) for a sample of 3 wt % and decreased with an increase of Ga_2O_3 content especially above 36 wt %.

Catalytic Test. The catalytic activities were measured at 773 and 823 K for the series of catalysts studied. To eliminate the influence of surface area, activity per surface area of the catalysts has been calculated and is shown in Figure 7. At the both reaction temperatures, the rate of NO reduction increased with an increase in Ga_2O_3 content up to around 27−36 wt % and decreased after that. It should be noted that the rate of CH_4 conversion also exhibited the maximum value at around 27−36 wt %, though the results are not shown.

Discussion

Validity of the Quantitative Structural Analysis by XANES. In our recent study,[12] the deconvolution analysis of Ga K-edge XANES was shown to be a novel method to quantify the gallium coordinations in various Ga_2O_3 catalysts. In this study, the same method was applied to the determination of the local structure of Ga_2O_3/Al_2O_3. Since the method is a simple phenomenalistic analysis, first we will discuss the validity of the quantitative analysis of Ga K-edge XANES. In Figure 8, the fractions of Ga(t) species calculated from XANES analysis are plotted versus those from EXAFS curve-fitting. Clearly, a proportional relationship was obtained with a slope of unity, indicating the substantial agreement between the results of XANES and EXAFS analysis. Thus, it is confirmed that the deconvolution analysis of Ga K-edge XANES is applicable to estimate the relative ratio of Ga species with tetrahedral and octahedral symmetries also in Ga_2O_3/Al_2O_3 samples.

Surface Structure of Ga_2O_3/Al_2O_3. The techniques used in this work indicated that the surface structure is clearly different between the samples with Ga_2O_3 content below 27 wt % and those above it. XRD analysis (Table 1) showed the absence of crystalline Ga_2O_3 below 27 wt % and the presence of the crystalline ϵ-Ga_2O_3 phase at higher content. From the BET surface area per gram of Al_2O_3 (Table 1), it is suggested that gallium oxide on Al_2O_3 is present as a thin-layer structure up to 27 wt %, while Ga_2O_3 particles are present at higher content. XPS results in Figure 1 suggested that the Al_2O_3 surface is covered by a uniform gallia thin-layer of thickness much less than the escape depth up to 27 wt %. A Ga_2O_3 content of 27 wt % corresponds to 14.8 Ga^{3+} nm^{-2}−Al_2O_3, which is very close to the number of the surface cation sites of γ-Al_2O_3(111) face (14.5 Al^{3+} nm^{-2}).[20] Therefore, it is considered that deposited

TABLE 2: Parameters of Deconvoluted Peaks in XANES Spectra of Ga_2O_3/Al_2O_3 and ss-Ga_2O_3

	Ga(t) species/eV			Ga(o) species/eV					
Ga_2O_3/wt %	position	FWHM	area	position	FWHM	area	Ga(t)+Ga(o) area	fraction of Ga(t)/%	fraction of Ga(o)/%
3	10375.5	3.0	5.0	10379.6	4.0	1.7	6.7	75	25
7	10375.5	3.1	4.8	10379.5	4.3	2.0	6.8	70	30
13	10375.5	3.2	4.5	10379.5	4.7	2.6	7.1	63	37
21	10375.5	3.1	4.3	10379.5	5.0	2.8	7.1	60	40
27	10375.2	3.1	4.1	10379.2	5.4	3.2	7.3	57	43
36	10375.6	3.2	4.0	10379.5	5.2	3.4	7.4	54	46
44	10375.7	3.2	3.9	10379.5	5.2	4.0	7.9	50	50
60	10375.6	3.2	3.5	10379.3	5.0	4.3	7.8	45	55
77	10375.6	3.2	3.4	10379.3	5.1	4.8	8.2	41	59
100	10375.2	3.6	3.1	10379.1	5.3	5.1	8.2	38	62
β-Ga_2O_3	10375.2	4.0	4.7	10379.6	4.0	4.7	9.4	50 (50)[a]	50 (50)[a]

[a] Values in parentheses are crystallographic data of β-Ga_2O_3.[18]

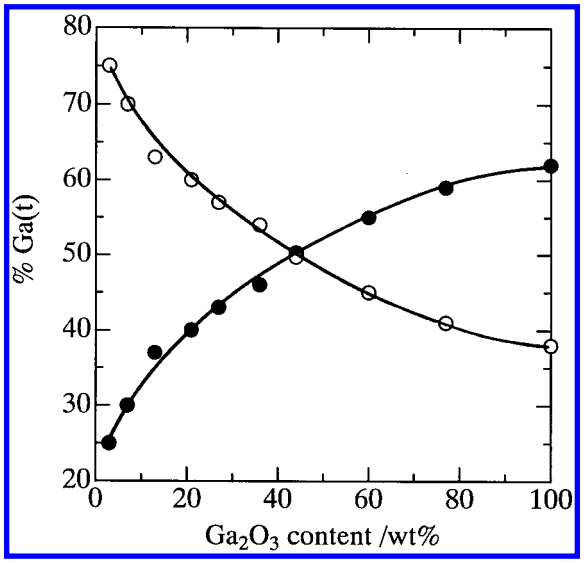

Figure 4. The fraction of Ga(t) species (○) and Ga(o) species (●) in Ga_2O_3/Al_2O_3 catalysts derived from the deconvolution analysis of Ga K-edge XANES.

gallium oxide is dispersed well over the Al_2O_3 surface, probably forming a monolayer up to 27 wt %.

XANES results (Figure 2) indicate that the local structure of samples below a monolayer coverage (27 wt %), dominantly containing tetrahedral Ga atoms, is different from that of bulk Ga_2O_3, and is very similar to that of the $Ga_2O_3-Al_2O_3$ mixed oxide, i.e., Ga species dispersed in Al_2O_3 matrix. In addition, EXAFS data (Table 3) showed that coordination numbers of the Ga−Al shell were around 6−7 for these samples. These results indicate that surface gallium oxide is strongly interacted with the Al_2O_3 support forming an aluminate-like structure as suggested in our previous study of Ga L_3-edge XANES.[11] Further, EXAFS data showed that the bond distances of Ga(t)−O and Ga(o)−O were almost constant for the samples below 27 wt % (R_t = 1.7 Å and R_o = 1.88 Å). These are shorter than the bond distances of β-Ga_2O_3 and are rather close to those of γ-Al_2O_3 (R_t = 1.72 Å and R_o = 1.95 Å).[28] From the above results, a consistent picture of the samples below 27 wt % is that gallium atoms are incorporated into surface cation sites of Al_2O_3 surface in monolayer thickness. This would be identical to the model called surface spinel.[22,29−31] Previously, Hercules et al. suggested for Ni/Al_2O_3 and Co/Al_2O_3 systems that the surface spinel is formed by a diffusion of cations during calcination into the surface cation sites of the Al_2O_3 where they occupy tetrahedral or octahedral sites.[31]

When Ga_2O_3 content exceeds the monolayer coverage, crystalline ϵ-Ga_2O_3 particles appear as described above. The

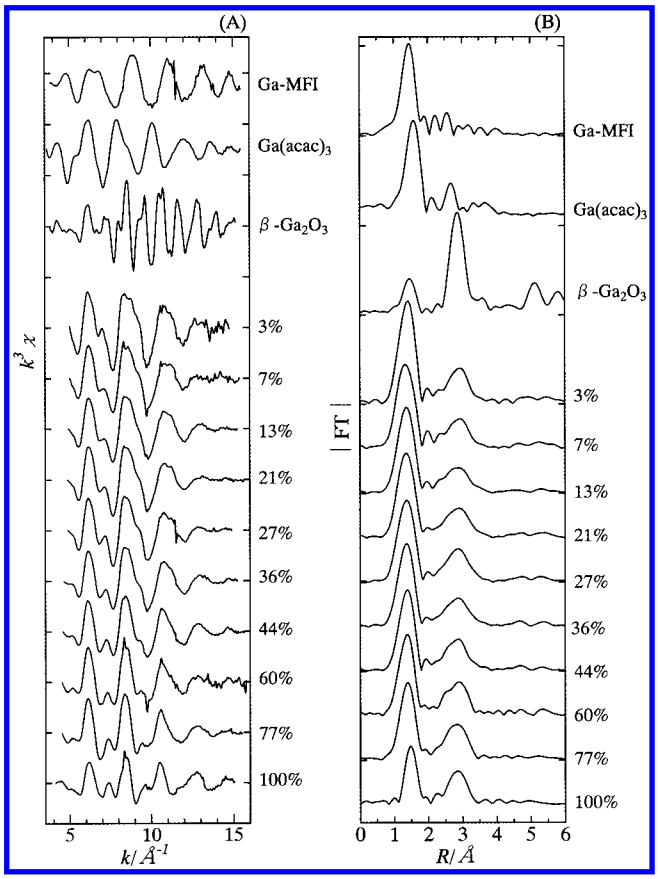

Figure 5. Ga K-edge EXAFS of Ga_2O_3/Al_2O_3 catalysts and reference compounds: (A) $k^3\chi(k)$ data; (B) radial structure function derived from Fourier transform of data shown in (A), not corrected for phase shift.

XANES result that the Ga(o) became predominant at high content would be due to the presence of the ϵ-Ga_2O_3 phase. From EXAFS data, above 36 wt %, the coordination numbers of the Ga−Al shell steeply decreased while those for the Ga−Ga shell did not, which implies the increase in Ga species which is not interacted with Al_2O_3. An increase in Ga−O distances with Ga_2O_3 content above 36 wt % should reflect that the Ga atom is not in the cation site of Al_2O_3, but in the Ga_2O_3 phase. It is considered that after Ga atoms saturate all available surface sites of Al_2O_3, Ga atoms can be accommodated only by formation of the ϵ-Ga_2O_3 phase. In fact, the presence of the separated Ga_2O_3 particle is observed in TEM micrographs of the 77 wt % sample. Thus, the drastic increase in the slope of XPS curve above 27 wt %, shown in Figure 1, can be explained as being due to the presence of this separated phase, which can

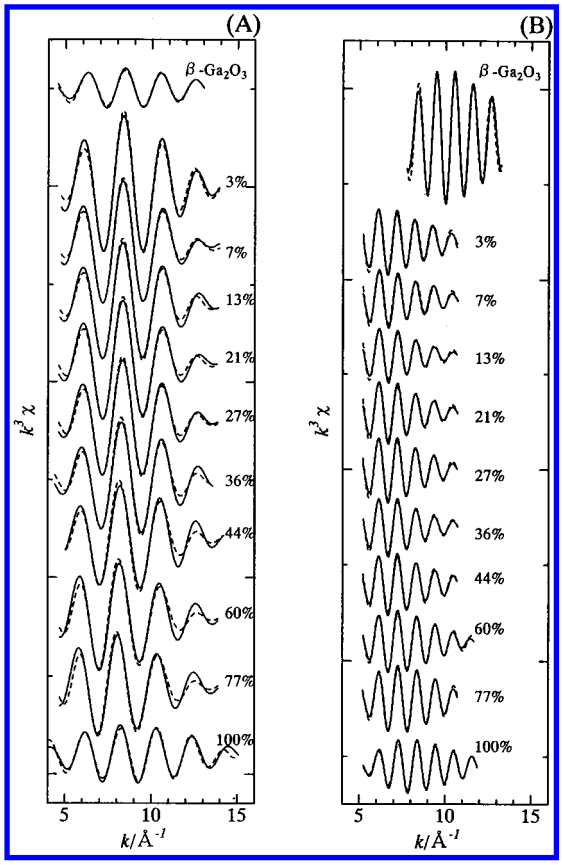

Figure 6. Fourier-filtered EXAFS function of Ga_2O_3/Al_2O_3 catalysts for the first shell (A) and for the second shell (B). (—) Experimental, (- - -) simulated.

exist outside and on the monolayer. A similar XPS curve was observed for the Co/Al_2O_3 system, where the increase in the slope was attributed to the presence of Co_3O_4 phase on the monolayer cobalt species.[22]

The detailed inspection of the XANES and EXAFS data below 27 wt % indicates that the structure of surface gallium atoms varies with Ga_2O_3 content even in monolayer thickness. For the 3 wt % sample, the coordination number of the Ga−Ga shell was the lowest (0.4) and that of the Ga−Al shell was the highest (7.2). This indicates that highly dispersed Ga atoms having Ga−O−Al bonds are incorporated in the surface of Al_2O_3. As Ga_2O_3 content increased, the coordination number for the Ga−Ga shell increased, and that for the Ga−Al shell decreases, suggesting that neighboring Al atoms are substituted by Ga atoms. The relative distribution of surface Ga species, i.e., Ga(t) and Ga(o), was also influenced by the Ga_2O_3 content as revealed by a quantitative analysis of XANES as shown in Figure 4. The fraction of Ga(t) was highest at the lowest Ga_2O_3 content (3 wt %) and decreased as Ga_2O_3 content increased. Previously, Navrotsky et al.[32] reported a strong preference of Ga^{3+} for tetrahedral sites relative to Al^{3+} in Al_2O_3 which was explained on the basis of crystal-field theory. This would result in a high Ga(t) fraction at low content. Since octahedral sites are also available, the percentage of Ga(o) increases as the surface concentration of Ga increases.

Active Site for the Selective Reduction of NO by CH_4. As shown in Figure 7, activity per surface area of Ga_2O_3/Al_2O_3 catalysts increased with an increasing amount of Ga_2O_3 up to around 27 wt % (monolayer coverage) and decreased at higher content. By considering the surface structure of Ga_2O_3/Al_2O_3 discussed above, this result clearly indicates that the surface spinel species is responsible for the activity toward the selective reduction of NO by CH_4, and the excess Ga_2O_3 particles contribute much less to the activity.

Below the monolayer coverage (27 wt %), it is assumed that all Ga atoms are present at the catalyst surface. Thus the set of samples allows us to calculate systematically the intrinsic catalytic activity of surface Ga atoms, differing in the local structure. Figure 9 shows the turnover frequency (TOF) defined as the rate of NO reduction divided by the number of surface Ga atoms. It is shown that TOF decreases as Ga content increases. This fact gives a circumstantial evidence of an inhomogeneity of the catalytic site, classified as a structure-sensitive reaction. Taking into account the result that the percentage of Ga(t) was also higher for the lower-content samples, it is clearly shown that TOF for NO reduction correlates well with the amount of Ga(t), but not with that of Ga(o). Therefore, it is concluded that the activity for NO selective reduction by CH_4 is sensitive to the coordination symmetry of the surface Ga atoms; tetrahedral Ga species in the surface spinel phase are responsible for the activity. This conclusion is consistent with our preliminary finding that low-coordinated Ga atoms are responsible for higher activity.[11] In addition, if we estimate TOF as the activity per surface Ga(t) species by assuming that the activity of Ga(o) species can be negligible, the TOF is the highest for the 3 wt % sample and decreases with Ga content. This may suggest that highly dispersed Ga(t) species having Ga−O−Al bonds, which exist more on the lower content samples (Table 3), exhibits high activity.

The question arises as to why tetrahedral Ga is the active species. Structure-sensitivity should occur if the rate-determining step demands a specific structure. Cant et al. showed, on the basis of the isotopic effect of CH_4 and CD_4 on Co-ZSM-5 catalysts, that the rate-determining step in SCR by CH_4 is the breaking of a C−H bond of a CH_4 molecule.[33] Miyamoto et al. studied the nature of the Ga site on Ga-ZSM-5 by using a computational method and suggested that the Ga atoms are in the low-coordination state compared to the situation in α-Ga_2O_3 (octahedra) owing to the interaction with the zeolite framework.[34] They also suggested that the low-coordinated Ga site is responsible for dissociative adsorption of a CH_4 molecule, resulting in the high activity of Ga-ZSM-5 for SCR by CH_4.[35] Kazansky suggested, on the basis of H_2 and alkane adsorption studies on Al_2O_3 and zeolites, that low-coordinated cation site with covalence in nature are required for dissociative adsorption of nonpolar molecules.[36] In our recent study, it was suggested that the positive shift of Ga K-edge peak energy is due to the increase of electronegativity of the ligand with an increase of the oxygen coordination number of Ga.[12] This implies that the Ga(t)−O bond is more covalent than the Ga(o)−O bond. Assuming that CH_4 activation is important for this reaction, one interpretation to the present conclusion is that the tetrahedral Ga atom, having the low-coordinated state and covalent nature, is required to activate CH_4, leading to the high activity for NO selective reduction by CH_4. The role of Al_2O_3 matrix should include the ability to act as a macroligand, providing Ga atoms in the low-coordinated and covalent tetrahedral environment.

Conclusion

Ga atoms on Al_2O_3 in different coordination symmetries (tetrahedral and octahedral) are quantitatively distinguished by Ga K-edge XANES deconvolution analysis, which has been confirmed by EXAFS curve-fitting analysis.

A variety of spectroscopic techniques have distinguished quantitatively the gallium oxides with different structures as a

TABLE 3: EXAFS Curve-Fitting Results[a] of Ga_2O_3/Al_2O_3 Samples and β-Ga_2O_3

	Ga(t)−O		Ga(o)−O		Ga−Ga		Ga−Al		
Ga_2O_3/wt %	N_t	R_t/Å	N_o	R_o/Å	N	R/Å	N	R/Å	% Ga(t)[b]
3	3.9	1.69	2.2	1.87	0.4	3.21	7.2	3.34	73
7	3.0	1.70	2.4	1.87	1.1	3.21	6.7	3.32	65
13	3.3	1.70	2.4	1.88	2.7	3.20	6.3	3.31	73
21	3.2	1.70	2.8	1.88	3.0	3.20	6.7	3.30	63
27	2.8	1.70	3.0	1.88	3.9	3.20	6.0	3.32	59
36	2.7	1.72	3.1	1.88	4.9	3.20	4.4	3.30	56
44	2.2	1.73	3.5	1.92	4.8	3.19	3.6	3.30	49
60	2.6	1.73	4.1	1.94	5.9	3.18	1.4	3.30	49
77	2.2	1.74	5.7	1.95	6.2	3.18	0.7	3.30	36
100	1.8	1.88	3.7	2.00	6.1	3.16	3.0[d]	3.40[d]	41
β-Ga_2O_3	1.6 (2.0)[c]	1.86 (1.83)[c]	2.6 (3.0)[c]	2.02 (2.00)[c]	6.1 (6.0)[c]	3.19 (3.06)[c]	6.9[d] (7.0)[c,d]	3.39[d] (3.34)[c,d]	50 (50)[c]

[a] N is coordination number; R is interatomic distance. [b] Fraction of Ga(t) species calculated by the following equation: $[(N_t/4)/((N_t/4 + N_o/6)] \times 100$. [c] Values in parentheses are crystallographic data of β-Ga_2O_3.[18] [d] Ga−Ga shell.

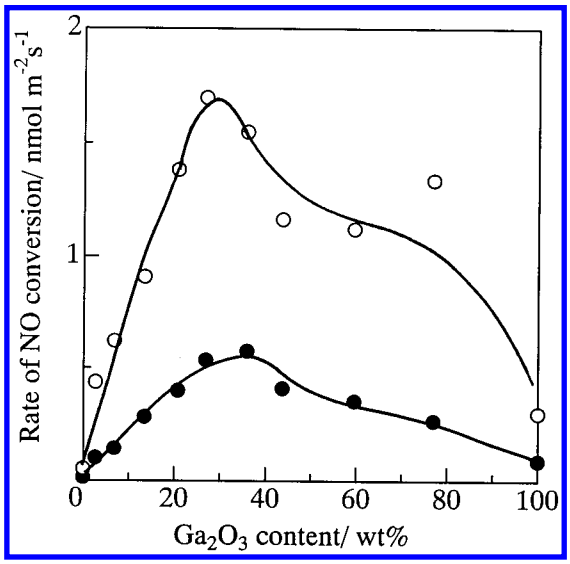

Figure 7. Catalytic activities of Ga_2O_3/Al_2O_3 catalysts for NO selective reduction by CH_4: the rate of NO conversion at 773 K (●) and 823 K (○) as a function of Ga_2O_3 content.

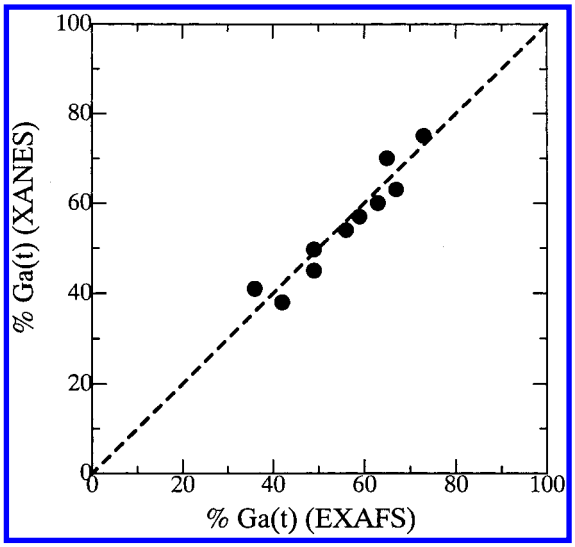

Figure 8. A plot of the fraction of Ga(t) species derived from the deconvolution analysis of XANES versus that from the curve-fitting analysis of EXAFS.

function of Ga_2O_3 content. Below monolayer coverage (27 wt %), Ga atoms are present at the surface cation site of Al_2O_3 support, in the form of the surface spinel phase. The difference

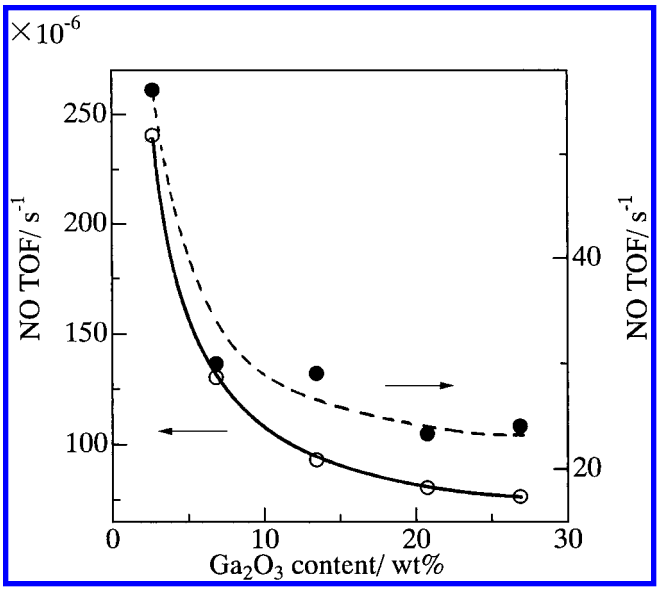

Figure 9. Turnover frequency for NO conversion at 773 K (●) and 823 K (○) as a function of Ga_2O_3 content.

in geometric coordinations within the surface spinel also depend on Ga_2O_3 content. At low content Ga atoms are located predominantly at tetrahedral sites of the Al_2O_3 surface, and the fraction of octahedra increases as the surface concentration of Ga increases. Above monolayer coverage, crystalline Ga_2O_3 particles are formed because they cannot interact with Al_2O_3 once the surface cation sites have been filled.

The coordination symmetry and surrounding matrix have a significant influence on the catalytic activity of surface Ga ions for NO selective reduction by CH_4. This reaction is a structure-sensitive reaction depending on the local structure of the Ga ion; GaO_4 tetrahedra highly dispersed in the surface spinel phase are responsible for the activity. The Al_2O_3 matrix would provide stabilization of Ga ions in the tetrahedral environment.

Acknowledgment. The X-ray absorption experiment was performed under the approval of the Photon Factory Program Advisory Committee (Proposal No. 96G-002). The authors thank Mr. H. Ishikawa of Toho Gas Co., Ltd. for his technical assistance on XPS measurement.

References and Notes

(1) Iwamoto, M.; Yahiro, H. *Catal. Today* **1994**, *22*, 5.
(2) Shelef, M. *Chem. Rev.* **1995**, *95*, 209.

(3) Armor, J. N. *Catal. Today* **1995**, *26*, 147.
(4) Armor, J. N. *Catal. Today* **1996**, *31*, 191.
(5) Kikuchi, E.; Yogo, K. *Catal. Today* **1994**, *22*, 73.
(6) Shimizu, K.; Satsuma, A.; Hattori, T. *Appl. Catal. B* **1998**, *16*, 319.
(7) Shimizu, K.; Maeshima, H.; Satsuma, A.; Hattori, T. *Appl. Catal. B* **1998**, *18*, 163.
(8) Bethke, K. A.; Kung, M. C.; Yang, B.; Shah, M.; Alt, D.; Kung, H. H. *Catal. Today* **1995**, *26*, 169.
(9) Hamada, H. *Catal. Today* **1994**, *22*, 21.
(10) Loughran, C. J.; Resasco, D. E. *Appl. Catal. B* **1995**, *7*, 113.
(11) Shimizu, K.; Takamatsu, M.; Nishi, K.; Yoshida, H.; Satsuma, A.; Hattori, T. *Chem. Commun*. **1996**, 1827.
(12) Nishi, K.; Shimizu, K.; Takamatsu, M.; Yoshida, H.; Satsuma, A.; Tanaka, T.; Yoshida, S.; Hattori, T. *J. Phys. Chem. B*, in press.
(13) Murakami, Y. *Stud. Surf. Sci. Catal.* **1983**, *16*, 775.
(14) Fung, S. C. *J. Catal*. **1979**, *58*, 454.
(15) Inumaru, K.; Okuhara, T.; Misono, M. *J. Phys. Chem.* **1991**, *95*, 4826.
(16) Penn, D. R. *J. Electron Spectrosc. Relat. Phenom*. **1976**, *9*, 29.
(17) Scofield, J. H. *J. Electron Spectrosc. Relat. Phenom*. **1976**, *8*, 129.
(18) Geller, S. *J. Chem. Phys.* **1960**, *33*, 676.
(19) The number density of Al atom in Al_2O_3 (40.1 nm^{-3}) was calculated from the bulk density of Al_2O_3 (3400 kg m^{-3}).
(20) Knozinger, H.; Ratnasamy, P. *Catal. Rev. Sci. Eng*. **1978**, *17*, 31.
(21) Nomura, M.; Koyama, A. *KEK Report 89-16*, **1989**.
(22) Chin, R. L.; Hercules, D. M. *J. Phys. Chem*. **1982**, *86*, 360.
(23) Dymock, K.; Palenik, G. J. *Acta Crystallogr. B* **1974**, *30*, 1364.
(24) Stave, M. S.; Nicholas, J. B. *J. Phys. Chem.* **1995**, *99*, 15046.
(25) *X-ray Absorption Fine Structure for Catalysts and Surfaces*; Iwasawa, Y., Ed. World Scientific: Singapore, 1996; Chapter 8.
(26) Teo, B. K. *EXAFS: Basic and Principles and Data Analysis*; Springer-Verlag: Berlin, 1986; Chapter 6..
(27) Rehr, J. J.; de Mustre, L.; Zabinsky, S. I.; Albers, R. C. *J. Am. Chem. Soc*. **1991**, *113*, 5135.
(28) Tachikawa, H.; Tsuchida, T. *J. Mol. Catal*. **1995**, *96*, 277.
(29) Jacono, M. Lo; Schiavello, M.; Cimino, A. *J. Phys. Chem.* **1971**, *75*, 1044.
(30) Wu, M.; Hercules, D. M. *J. Phys. Chem*. **1979**, 83, 2003.
(31) Bruggraf, L. W.; Leyden, D. E.; Chin, R. L.; Hercules, D. M. *J. Catal*. **1982**, *78*, 360.
(32) Navrotsky, A.; Kleppa, O. J. *J. Inorg. Nucl. Chem*. **1967**, *29*, 2701.
(33) Cowan, A. D.; Dumpelmann, R.; Cant, N. W. *J. Catal*. **1995**, *151*, 356.
(34) Miyamoto, A.; Himei, H.; Oka, Y.; Maruya, E.; Katagiri, M.; Vetrivel, R.; Kubo, M. *Catal. Today* **1994**, *22*, 87.
(35) Himei, H.; Yamadaya, M.; Kubo, M.; Vetrivel, R.; Broclawik, E.; Miyamoto, A. *J. Phys. Chem.* **1995**, *99*, 12461.
(36) Kazansky, V. B. In *Acidity and Basicity of Solids*; Fraissard, J., Petrakis, L., Eds.; Kluwer Academic Publishers: Dordrecht, 1994; p 199.